# Simulation of train-turnout interaction and validation using field measurements

Wan, C; Markine, VL; Shevtsov, IY

**DOI**
10.4203/ccp.98.136

**Publication date**
2012

**Document Version**
Accepted author manuscript

**Published in**
Proceedings of the international conference on railway technology: Research, development and maintenance

# Simulation of Train-Turnout Interaction and Validation using Field Measurements

**C. Wan*, V.L. Markine* and I.Y. Shevtsov****

* Section of road and Railway Engineering
Faculty of Civil Engineering and Geosciences
Delft University of Technology, The Netherlands

** ProRail, Utrecht, The Netherlands

v.l.markine@tudelft.nl

## Abstract

The dynamic behaviour of different turnouts has been analysed using the finite element model. The vertical rail geometry of the common crossing has been obtained using the image of the crossing nose and the measured rail geometry. The train-turnout interaction has been simulated for three turnouts from the Dutch railway network.

The simulation results have been compared with the measurement data obtained from the instrumented crossing nose of the corresponding turnouts. The comparison concentrating on the time history of the vertical accelerations of the crossing nose has shown that the results of the simulations are in good agreement with the measurements. From these results it can be concluded that the model is able to simulate the train-turnout interaction with good accuracy. Also, the possibilities of tuning the model are discussed in the paper.

**Keywords:** train-turnout interaction, rail geometry, numerical simulation, instrumented turnout, field measurements, model validation.

## 1 Introduction

Railway turnouts (switches and crossings) are essential components of the railway infrastructure which provide flexibility of the system by enabling railway vehicles to be switched from one track to another at a railway junction. Due to the rapidly varying wheel-rail contact geometry and changes of track flexibility, very high contact forces can occur during wheel passing over the switch toe and the crossing,

producing local damage of the contact surfaces as well as transmitting noise and vibrations to the environment. According to [1], the impact loads acting on the crossing nose can be several times higher than the static wheel load. Therefore the train-track interaction is of high importance in turnout designs and maintenance of railway systems.

To estimate the train-turnout interaction a special attention should be paid to the discontinuity in the rail geometry which contributes the major rail excitations. Several numerical procedures have been proposed recently focusing on modelling the continuously changing track geometry such as rail with various cross-sections and sleepers varying in length along the crossing, to account for the complicated geometric effect and elasticity-related effects on dynamic response of a turnout.

Various three dimensional (3-D) simulation methods haven been used to analyse the dynamic response of the turnout. In [2], the dynamic interaction between a railway vehicle and a turnout has been simulated using the commercial multi-body system software GENSYS and a home-developed package DIFF3D. The simulation results have been compared with each other and validated through full scale field tests [3]. In [4] the dynamic simulation package VAMPIRE® has been developed to determine the wheel impact forces when train passing a turnout. A flexible track model and the real-time wheel–rail contact model in NUCARS® have been used for a tread bearing diamond crossing design study [5]. The multi-body simulation package SIMPACK has been used to calculate the vehicle dynamic behaviours when passing over a turnout [6,7]. A mathematical model accounted for the effects of rail profile variation along the track and of local variation of track flexibility has been proposed in [8] to simulate the train-turnout interaction; the results have been compared with the experiments. However, high computational effort is required when using the abovementioned 3-D simulation methods, especially when the turnout is modelled as the flexible track.

Recently, numerical optimisation methods have been used to achieve the optimum dynamic performance of the turnout by tuning the parameters of the train-turnout system [9,10], showing that numerical optimisation has the significant potential to improve the dynamic properties of the track system. Usually, in such a practical optimisation multiple numerical analyses are involved and the total computational costs of such an optimisation might become prohibitive when using the computationally expensive numerical analyses. Therefore less time consuming computational methods are preferable in it in the numerical optimisation process.

To obtain a turnout model that could be further used in the numerical optimisation process the computer package DARTS_NL (TU Delft) for fast dynamic vehicle–track analysis has been used. To allow for validation of the developed numerical model, field measurements were performed on several instrumented turnouts to collect response data when trains passing through. In Section 2 the numerical model of dynamic train-turnout interaction is described. The setup of field measurements on instrumented turnouts is introduced in Section 3. The comparison of the measured and the simulated results is presented in Section 4, followed by the discussion of the improvement of the model. Section 5 summarizes the main conclusions and remarks.

# 2 Numerical model of train-turnout interaction

## 2.1 Train-track interaction in DARTS_NL

The software DARTS_NL has been specially developed for the analysis of a rail track on an elastic foundation. In order to reduce the computational effort the modelling in DARTS_NL is restricted to two dimensions (the vertical and longitudinal directions) while using linear material property elements. The modelling approach is based on the coupling of the finite model of the track and the finite model of the moving train.

The track structure is modelled using a series of alternating stiff and soft layers. Each stiff layer consists of Timoshenko beam elements while the elastic layers are represented by distributed spring and damper combinations (Kelvin elements) as shown in Figure 1.

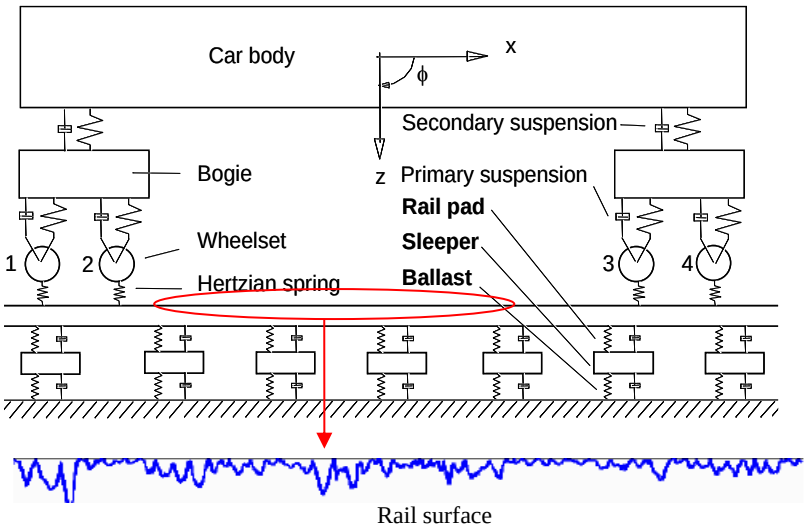


Figure 1: Model of ballast track structure and railway vehicle

A train model contains one or several wagons. Each wagon is represented by a mass-spring system that consists of four wheels, two bogies and a car body, which are modeled as rigid bodies and connected to each other by the primary and secondary suspensions (Kelvin elements). It is assumed that all components are in ideal service condition, no wheel irregularities are included in the train model.

The contact forces between the wheel and rail are modelled using the non-linear Hertzian spring with the stiffness [11].

$$K_H = \sqrt[3]{\frac{6E^2 P\sqrt{R_w R_r}}{4(1-\nu^2)^2}} \tag{1}$$

Where

$P$ is the static wheel load

$R_w$ and $R_r$ are the radii of the wheel and rail profile (the lateral cross-section)

$E$ is the Young modulus of the wheel and rail material

$\nu$ is the Poisson coefficient.

A moving vehicle generates the dynamic load due to the roughness of the rail surface (Figure 1). Therefore proper representation of the track geometry in the numerical model is essential for realistic simulation of the train-track interaction. In DARTS_NL the vertical rail geometry, that is the rail surface, can be defined either as a periodic function or as a numeric data profile obtained from measurements.

The train-track interaction is performed in the time domain following the concept of the displacement method. The main steps in the numerical procedure are:

- Assembling the mass $\mathbf{M}$, damping $\mathbf{C}$ and stiffness $\mathbf{K}$ matrixes and the vector of the external forces $\mathbf{f}$
- Generation of the equations of motion

$$\mathbf{M}\ddot{\mathbf{u}} + \mathbf{C}\dot{\mathbf{u}} + \mathbf{K}\mathbf{u} = \mathbf{f} \tag{2}$$

- Solution of the equations of motion yielding displacement vector $\mathbf{u}$ and acceleration $\ddot{\mathbf{u}}$
- (Optional) filtering of the obtained displacements vector $\mathbf{u}$ and acceleration $\ddot{\mathbf{u}}$ by cutting off the high frequency contributions
- Calculation of responses including forces in each track layer, contact forces and accelerations of rail and wheel based on the (filtered) displacements $\mathbf{u}$.

## 2.2 The turnout model

To assess the accuracy and reliability of the DARTS_NL model, the passenger trains negotiating the turnouts varying in crossing angle, rail geometry and service condition have been considered. The results are to be compared with corresponding field measurements.

Depending on the real case, the turnout structure is modelled using a series of alternating hard and soft layers. Here relatively hard rail pads (stiffness: 3032 MN/m, damping: 29 kNs/m) are used in the model representing the connection of rail and sleepers.

It should be noted that DARTS_NL uses symmetry of a track in the vertical plane thus only half of the track is represented in the model. While for a turnout, the rail, rail support and vertical rail geometry on the inner and outer side are not the same (a normal rail on the outer side and the crossing on the inner side). Therefore, some

dynamic effects such as rolling of the vehicle are ignored, which is allowable in terms of relative and qualitative analysis. Since the inner part including the crossing nose is more sensitive to damages, it is representative to consider this part in the analysis of the train-turnout interaction. Moreover, in [4] it was shown that the vertical impact forces are not significantly different when train passes the turnout in the main or divergent direction. allowing to consider only the main direction in simulation with the two dimensional model. In order to analyse the dynamic response of the crossing, the inside half of the through rail of the turnout has been modelled (Figure 2). The rail support has been modelled using four layers representing rail, rail pads, sleepers and ballast bed respectively.
Turnout with different angle and different length have been modelled according to the standard design of the turnouts. For 1:12 turnout, the total length is 54 m with 7 m representing the crossing, while for 1:15 turnout, 72 m in total with 9 m as the crossing.

Figure 2Figure 2 sketches a typical right hand turnout. The turnout is modelled with variable rail cross-sections and sleepers varying in length, based on the corresponding design drawings. The detailed modelling approach can be found in [1].

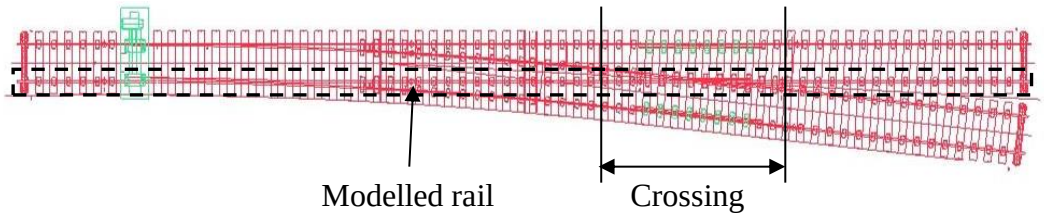


Figure 2: Turnout with crossing angle 1: a

In the model, the vertical rail geometry of the turnouts has been created based on the combination of the visual image of the turnout that provides the information of the transition zone, and the measured geometry data (the vertical distance from the top of the wing rail to the crossing nose) along the crossing. As shown in Figure 3, the location and length of transition zone where wheel travels from wing rail to the crossing nose, can be obtained from the visual image of the turnout (Figure 3a). The vertical gap between the crossing nose and the wing rails depends on the measured rail geometry data along the crossing (Figure 3b), which determines the vertical dip at the end of the transition zone. Then the geometry of the turnout can be defined (Figure 3c).

It should be noted that, due to the two dimensional restriction and simplifications of DARTS_NL model, the wheel is assumed to move through the turnout completely guided by the given rail geometry, that is, the wheel trajectory will be the same as the vertical rail geometry.

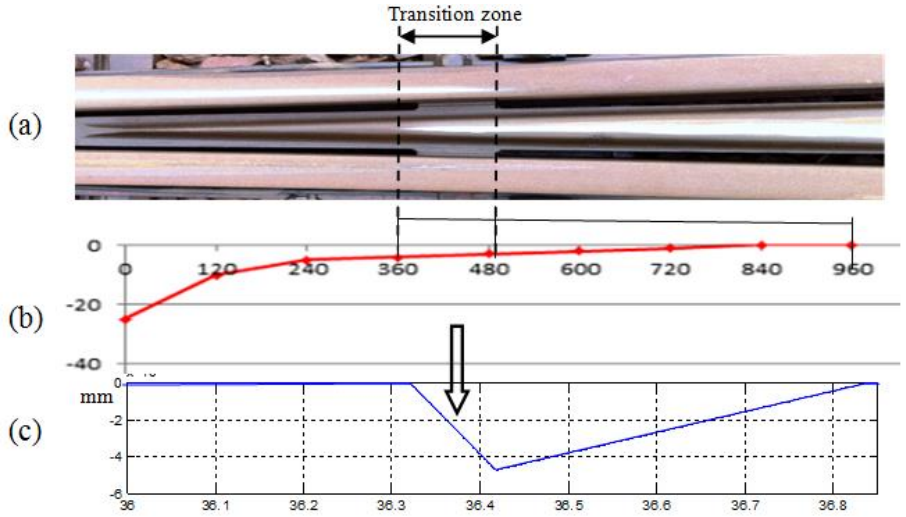


Figure 3: Creation of vertical rail geometry of turnout in the model: (a) image of the turnout, (b) measured geometry of the crossing nose (the nose point is the 0 point), (c) rail geometry in the model

The real wheel trajectory would change if the wheel load or the speed of the train changes. For a certain turnout, the higher the speed is, the farther the transition zone can be away from the tip of the crossing nose. Meanwhile, the shape of the trajectory also differs according to loading conditions [12]. However the transition zone in the images of the turnout (Figure 3a) correspond to the typical velocity, and in the simulations the velocities are the typical velocities of the turnouts. Thus the effect of the train velocity is included.

# 3 Setup of field measurement

The measured turnouts are UIC54 E1 turnouts. The measurement device has been used to record the acceleration signal and the train speed. The three-dimensional acceleration sensor has been mounted on the crossing rail a certain distance from the nose point close to the end of the transition zone (see Figure 4). It is expected that the major dynamic impacts occur around that point. The placement of the sensor depends on the travelling direction.


Figure 4: setup of measurement for acceleration of crossing nose

The speed measurement device consisting of 2 inductive sensors has been installed on the rail before the nose point. The distance between the two inductive sensors is 1 m.

It is worthwhile to mention that, neither the test trains nor the traveling velocities were pre-designated, but totally depended on the real traffic situation of the line. i.e. the measurement would be done when any train passes through the turnout in the main facing direction. At the same time, the type and basic information of the trains were written down of which the detail parameters can be found in the train database later. In this way the validation of the model could be more reliable.

# 4 Comparison of measured and simulated results

Numerical results from the DARTS_NL models are compared with the corresponding field measurements. Two 1:12 turnouts and a 1:15 turnout have been measured and modelled in DARTS_NL, thus three validation cases characterised by different turnouts and different load conditions are considered here.

## 4.1 The 54E1- 1:12 turnout case

The first case used for validation refers to the 54 E1 1:12 turnouts (turnout A and turnout B) on ballast bed. The measurements have been performed on site for two turnouts near a train station, which means that the train velocity was not constant due to the accelerating and braking of the train.

In the location of the crossing nose, the railway wheel encounters a discontinuity in the rail geometry, which is responsible for the shape and amplitude of acceleration of the crossing nose. The vertical distance from the top of the wing rail to the crossing nose have been measured every 12 cm along the crossing to adjust the vertical rail geometry in the numerical model. The measured rail geometry is presented in Figure 5, it can be seen that due to wear the geometries of both turnout crossings are slightly different from the designed one.

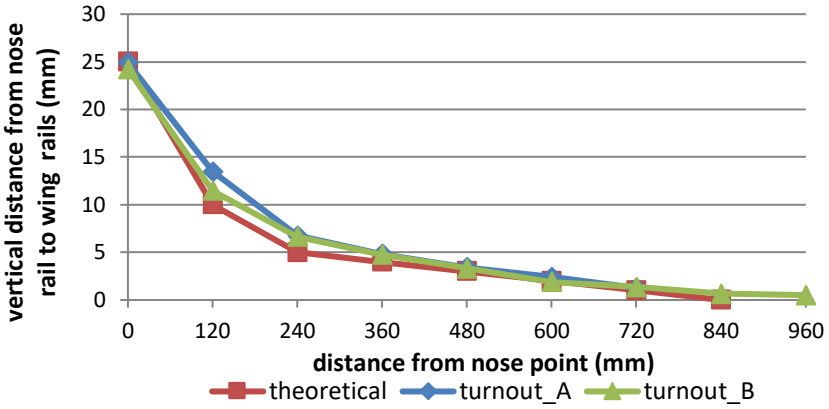


Figure 5: Measured rail geometry of 1:12 turnout

Based on the image of the turnout and the measured rail geometry, the vertical geometry of the two turnouts has been obtained according to the procedure described in Section 2.2 (Figure 3) as shown in Figure 6 and Figure 7, where the nose point locates at 36.0 m in the model.

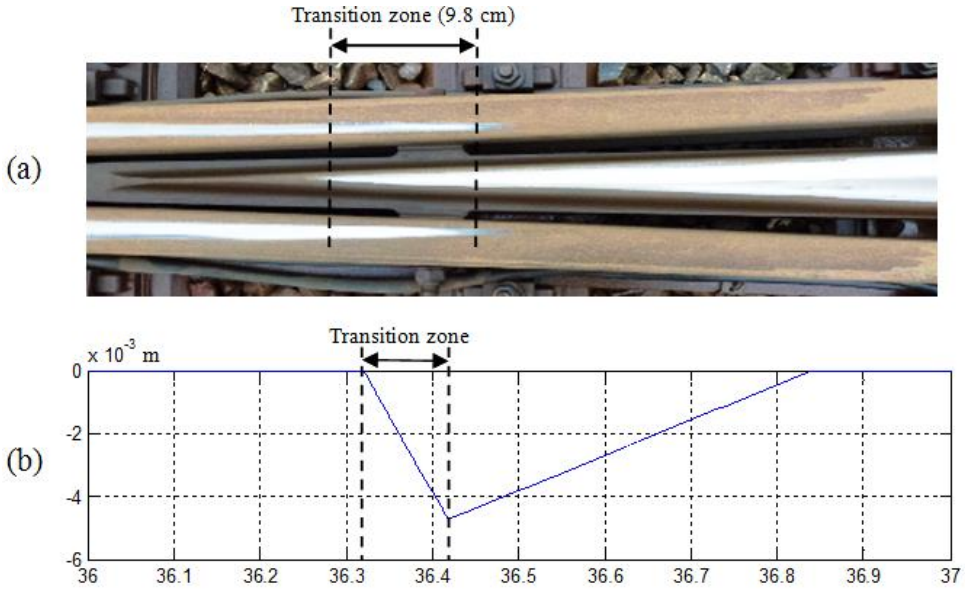


Figure 6: Creation of vertical rail geometry of turnout A in the model: (a) image of the turnout, (b) vertical geometry in the model

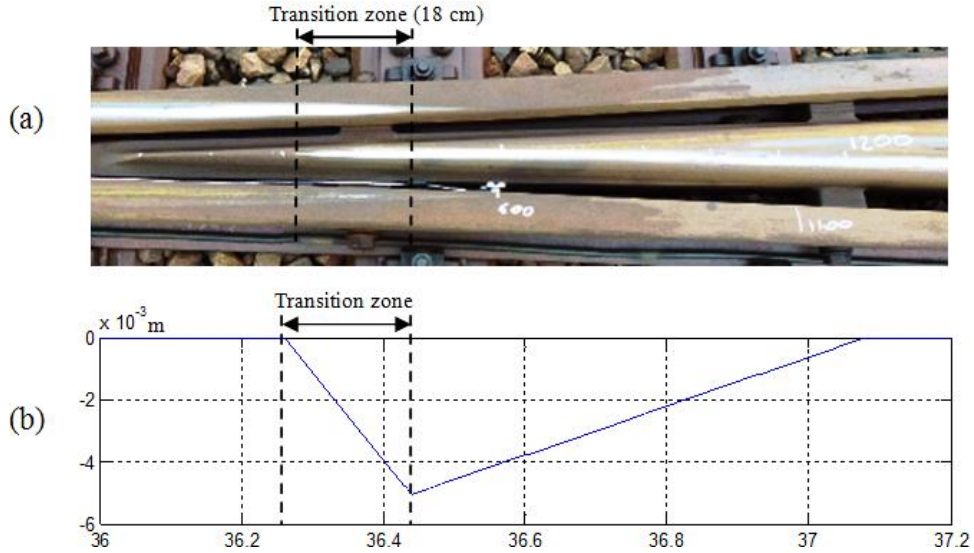


Figure 7: Creation of vertical rail geometry of turnout B in the model: (a) image of the turnout, (b) vertical geometry in the model

The measured time histories of the vertical acceleration of the crossing nose during train passage at 80 km/h on turnout A and 87 km/h on turnout B have been compared with the simulations. The measured train on turnout A has four 4-axle coaches (axle load 71.2 kN) with 2.5 m between the wheelsets and 20 m between the center of front and rear bogie. In the turnout B case, the train has five 4-axle coaches with the same axle load as that of turnout A. For the sake of clarity and simplicity, the comparison has been performed for one bogie of the train passing through the turnout over the time interval of 0.3 s (Figure 8 and Figure 9). By comparing these measurements and simulations, it can be found that for both turnouts, the main response of the crossing nose has been described correctly in the model.

Figure 8Figure 8a reports the time history of the measured vertical acceleration at the crossing nose of turnout A, wherein a single large impact ([1] and Figure 9) is replaced by two smaller impacts. This is mainly due to the fact that the turnout has just been repaired. While the simulation (Figure 8b) results in a single impact followed with the small vibrations damped out gradually with time. It can be explained by the fact that for the model the vertical geometry of the turnout crossing is simplified as two linearly changing parts with a dip at the end of the transition zone (Figure 6), thus only a major impact has been presented. When looking at the extreme values of the acceleration the maximum amplitudes are almost 1.5 times of the measurement, as presented in Table 1. It could be due to the fact that the rail irregularities are not presented in the model and the single impact is replaced by the two smaller impacts.

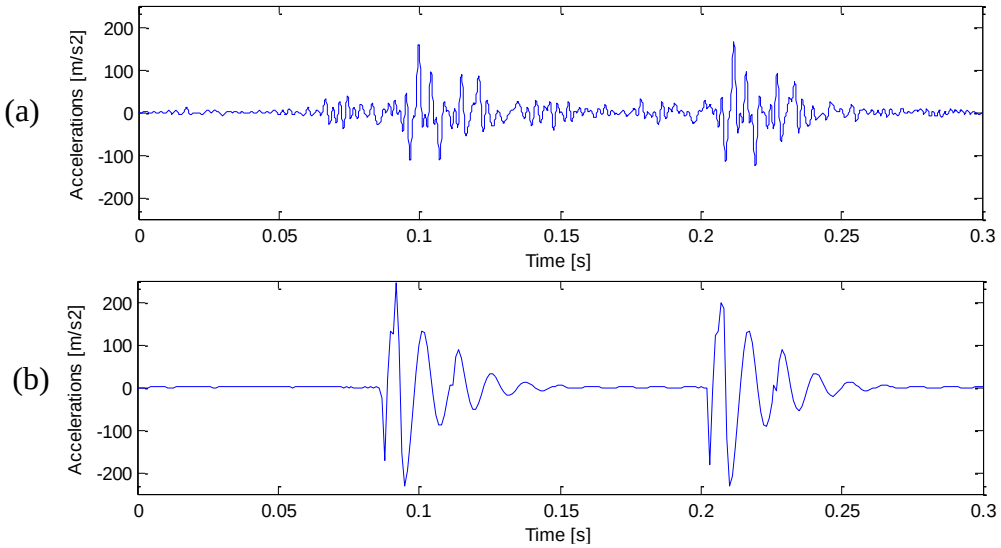


Figure 8: Results of turnout A—vertical acceleration at the crossing nose during the passage of a whole bogie (80 km/h): (a) field measurement, (b) simulation

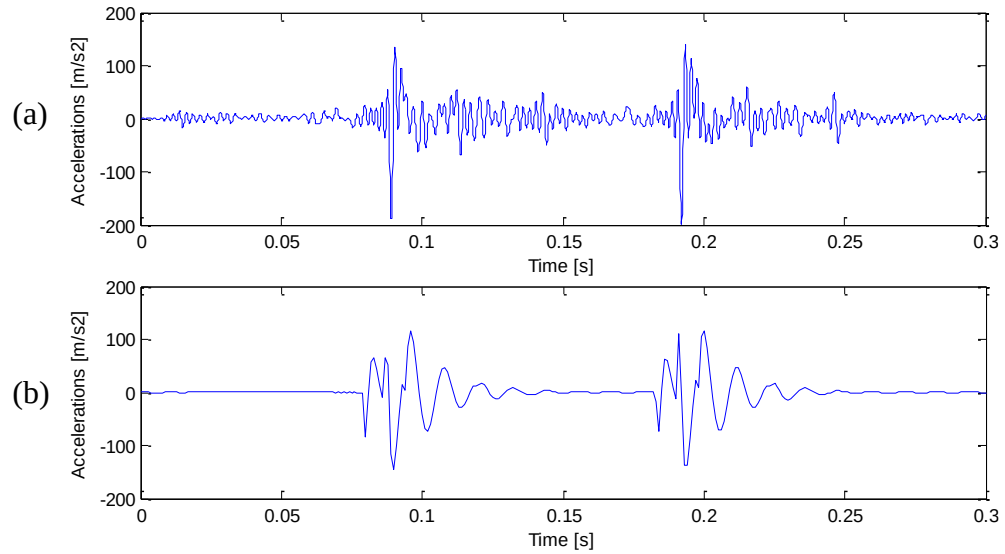


Figure 9: Results of turnout B—vertical acceleration at the crossing nose during the passage of a whole bogie (87 km/h): (a) field measurement, (b) simulation

| | Turnout A | | | Turnout B | | |
|---|---|---|---|---|---|---|
| Maximum amplitude | Measurement ($m/s^2$) | Simulastion ($m/s^2$) | M vs. S | Measurement ($m/s^2$) | Simulastion ($m/s^2$) | M vs. S (dB) |
| Positive | 159.7184 | 246.65 | 1:1.544 | 138.808 | 116.44 | 1:0.839 |
| Negative | -154.3677 | -230.07 | 1:1.490 | -197.714 | -145.66 | 1:0.737 |

Table 1: Comparison of the amplitude of the vertical acceleration at the crossing nose of 1:12 turnouts

Figure 9 reports the measured and simulated vertical acceleration of the crossing nose of turnout B. In the measurement (Figure 9a) the impact produced by the wheel passage, is well recognisable, although less predominant as compared to the random effect produced by rail irregularities. This could be because of the better geometric condition of the turnout, which is a newly installed one. The computed vertical acceleration signal (Figure 9b) is slightly different from the measured response, the extra vibrations due to rail irregularities are not present in the simulation, since the rail irregularities were not considered in the simulation due to lack of information about the actual geometry of the railhead along the turnout. Nevertheless, in the simulated results the major impact has the shape similar to the measurement, and the extreme values are in good agreement with the measurement (Table 1).

Interesting is that, turnout A and turnout B are the same except the local geometry of the crossing, while the performance of turnouts is quite different, which demonstrates the importance of rail geometry in train-turnout interaction. The simulations for the two turnouts which are based on the turnouts images are also different and are in good agreement with the measurements. This means that the effect of rail geometry can be effectively accounted for in the numerical model.

## 4.2 The 54E1-1:15 turnout case

The second comparison also deals with the 54 E1 turnout on ballast bed (turnout C), while the crossing angle is 1:15. The measurements have been performed when trains were passing the turnout in the main facing direction.

As in the 1:12 turnout case, the vertical rail geometry has been measured for turnout C, which also shows certain difference as compared with the theoretically designed turnout (Figure 10). After that the vertical rail geometry for the turnout model has been obtained based on the image of turnout C and the measured rail geometry data, which is presented in Figure 11. To compare with the numerical simulation, the data from the measurements sampled at 10 kHz have been low-pass filtered with the cut-off frequency of 500 Hz.

Figure 12 depicts the time histories of the measured and simulated vertical acceleration of the crossing nose during the train passage at 130 km/h on turnout C. Herein the measured train has six 4-axle coaches with the axle load of 71.2 kN. The comparison is performed for the passage of one bogie over the time duration of 0.3 s. As it can be seen in Figure 12 the result of the simulation is very close to the measurement both in shape and in amplitude (Table 2), which indicates that the main behaviour of the turnout has been grasped in the model.

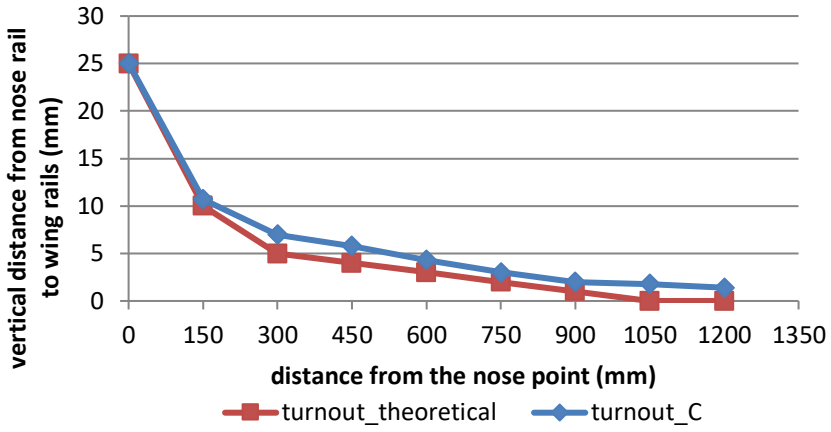


Figure 10: Measured rail geometry of 1:15 turnout (turnout C)

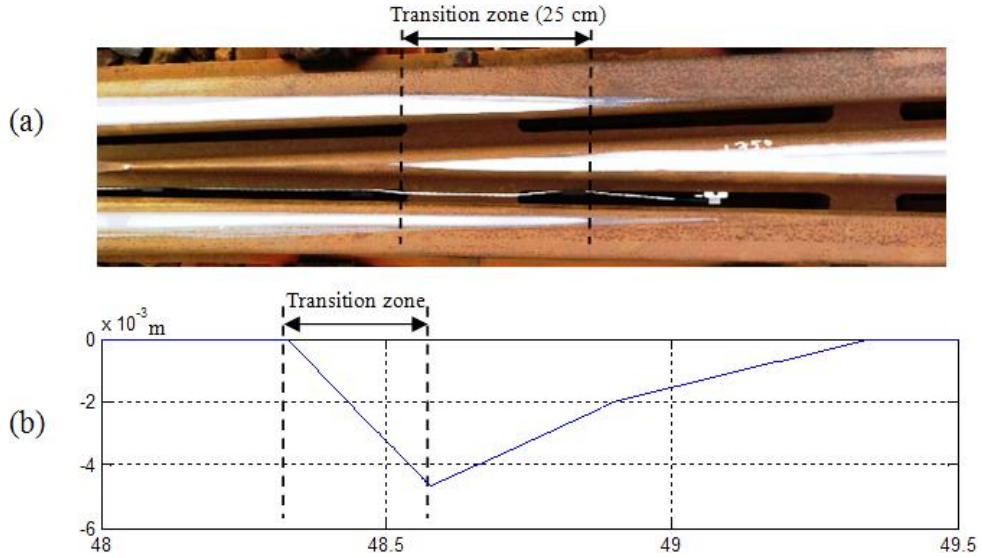


Figure 11: Creation of vertical rail geometry of turnout C in the model: (a) image of the turnout, (b) vertical geometry in the model

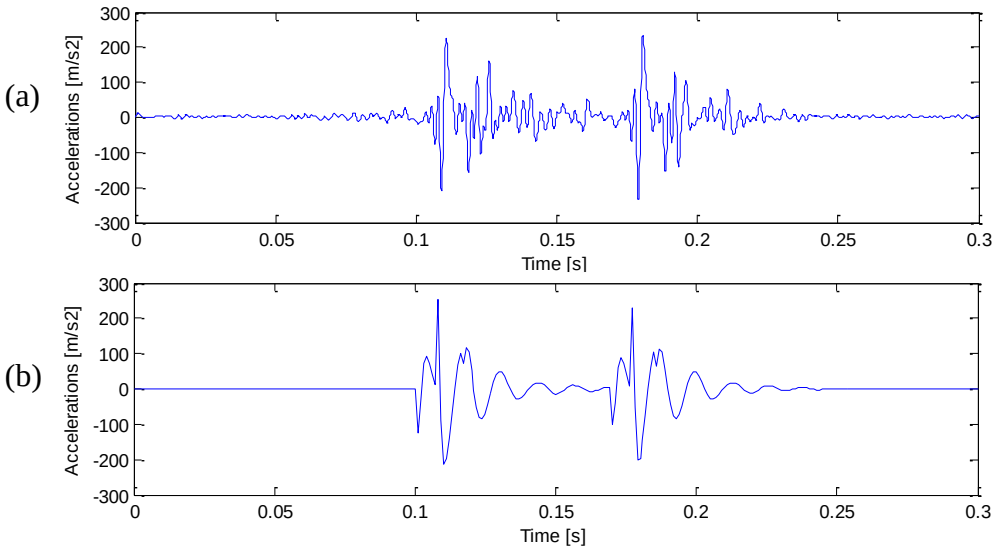


Figure 12: Results of turnout C—vertical acceleration at the crossing nose during the passage of a whole bogie (130 km/h): (a) field measurement, (b) simulation

| | Turnout C | | |
|---|---|---|---|
| Maximum amplitude | Measurement ($m/s^2$) | Simulastion ($m/s^2$) | M vs. S (dB) |
| Positive | 234.0274 | 254.7000 | 1:1.085 |
| Negative | -233.1764 | -215.0900 | 1:0.922 |

Table 2: Comparison of the amplitude of the vertical acceleration at the crossing nose of 1:15 turnout

It should be noted that the turnout has just been repaired after damage at the crossing nose, and therefore the measured rail geometry presents relatively larger difference as compared with the theoretical one as shown in Figure 10. Here the vertical rail geometry of the crossing after the transition zone is not linearly changing as in the case of the theoretical one. By using this measured geometry in the numerical simulations (Figure 11) the more accurate results have been obtained than when using only the theoretical crossing [1]. This again shows that the effect of rail geometry on turnout response can be well revealed.

## 4.3 Discussion of the model

From the above results, it can be concluded that the model is validated successfully and can be used in analysis of train-turnout interaction. The use of such a model can save a lot of computational effort compared with other complex numerical models, allowing it being utilized in numerical optimization of train-turnout interaction. However, it should be noted that the model has limitation when dealing with irregular wheel and rail geometry, which is the main factor contributing to the discrepancies from measurements.

To increase the accuracy of the model in such cases, more detailed 'rail surface' (section 2.1) could be applied in the model. This can be achieved through two main approaches, to use more detailed rail geometry including irregularities and to get more accurate wheel trajectory. The former can be realized by using instruments specialized in measuring rail geometry, so that the measured data can be used to generate the vertical geometry of the turnout. It was found from [12] that when using the wheel trajectory from 3-D multi-body model (Adams/Rail) as the vertical rail geometry of the turnout in DARTS_NL model, the results are very close to the 3-D dynamic simulations. This indicates that the model can simulate the response of the turnout during the passage of moving vehicles with the similar level of accuracy as the complex model.

# 5 Conclusion and remarks

The finite element model DARTS_NL used for simulation of the train-turnout interaction has been validated through the field measurements.

Three turnouts from the Dutch railway network varying in crossing angle, service state and load condition have been used as the validation cases. The simulation results are in good agreement with the measurements. The main behaviour of the turnouts has been correctly grasped of which the shape and extreme amplitudes of vertical acceleration of the crossing nose are close to the measurements.

The method of modelling the rail geometry using the visual image of the turnout introduced in [1] has further been developed here. The use of measured rail geometry together with the visual images of the crossing in obtaining the simplified rail geometry has been proposed. The simulation results have shown that the effect of vertical track geometry on the dynamic response of the turnout has been effectively accounted for in the model.

From these results it can be concluded that the model is able to simulate train-turnout interaction with high accuracy. The next step will include optimization of the turnout using the model.

# References


[1] V.L. Markine, M.J.M.M. Steenbergen, I.Y. Shevtsov, "Combatting RCF on Switch Points by Tuning Elastic Track Properties", Wear, 271(1-2), 158-167, 2011.

[2] E. Kassa, C. Andersson, J.C.O. Nielsen, "Simulation of Dynamic Interaction between Train and Railway Turnout", Vehicle System Dynamics, 44(3), 247-258, 2006.

[3] E. Kassa, J.C.O. Nielsen, "Dynamic Interaction between Train and Railway Turnout: Full-scale Test and Validation of Simulation Models", Vehicle System Dynamics, 46(supplement), 521-534, 2008.

[4] Y.Q. Sun, C. Cole, M. McClanachan, "The Calculation of Wheel Impact Force due to the Interaction between Vehicle and a Turnout", Proceedings of the

Institution of Mechanical Engineers, Part F: Journal of Rail and Rapid Transit , 224 (special issue), 391-403, 2010.

[5] X. Shu, N. Wilsona, C. Sasaoka, J. Elkins, “Development of a Real-time Wheel/rail Contact Model in NUCARS®1 and Application to Diamond Crossing and Turnout Design Simulations”, Vehicle System Dynamics, 44(supplement 1), 251-260, 2006.

[6] G. Schupp, C. Weidemann, L. Mauer, “Modelling the Contact between Wheel and Rail within Multibody System Simulation”, Vehicle System Dynamics, 41(5), 349-364, 2004.

[7] H. Netter, G. Schupp, W. Rulka, K. Schroeder, “New Aspects of Contact Modelling and Validation within Multibody System Simulation of Railway Vehicles”, Vehicle System Dynamics, 29(supplement 1), 246-269, 1998.

[8] S. Alfi, S. Bruni, “Mathematical Modelling of Train-turnout Interaction”, Vehicle System Dynamics, 47(5), 551-574, 2009.

[9] V.L. Markine, C. Wan, I.Y. Shevtsov, “Improving the Performance of a Turnout by Optimising its Vertical Stiffness Properties”, in Proceedings of the Thirteenth International Conference on Civil, Structural and Environmental Engineering Computing, B.H.V. Topping and Y. Tsompanakis, (Editors), Civil-Comp Press, Stirlingshire, United Kingdom, page 17, 2011, DOI:10.4203/ccp.96.17. ISBN 978-1-905088-46-1.

[10] B. Palsson, J.C.O. Nielsen, “Kinematic Gauge Optimization of Switches using Genetic Algorithms”, IAVSD 22nd International Symposium on Dynamics of Vehicles on Roads and Tracks, Manchester, United Kingdom, 2011.

[11] S.L. Grassie, “Dynamic Modelling of Railway Track and Wheelsets”, Proc. Second Int. Conf. Recent Advances Struct. Dyn., Inst. of Sound and Vibration Research, University of Southampton, 1984.

[12] C. Wan, V.L. Markine, “Analysis of Wheel-rail Interaction in Turnout Crossing”, Research assigned by ProRail, TU Delft report 7-12-234-01, 2012, ISSN 0169-9288.